Elastic scattering of two Na atoms

R. Côté and A. Dalgarno
Harvard-Smithsonian Center for Astrophysics, 60 Garden Street, Cambridge, Massachusetts 02138
(Received 31 May 1994)

Interaction potentials for the $X\,^1\Sigma_g^+$ and $a\,^3\Sigma_u^+$ states of Na_2 are constructed and used in calculations of the elastic scattering of two Na atoms at ultralow temperatures. The sensitivity to retardation effects (or Casimir corrections) is explored. The calculated elastic and spin-change cross sections are very large, of the order of 10^{-12}–10^{-13} cm^2 at zero temperature. The predicted scattering lengths are both positive, 34.9 a_0 for the $X\,^1\Sigma_g^+$ state and 77.3 a_0 for the $a\,^3\Sigma_u^+$ state. Pronounced shape resonances appear for the $l=3$ and 7 partial waves for the singlet and $l=6$ for the triplet states.

PACS number(s): 34.40.+n

I. INTRODUCTION

Collision processes at millidegrees Kelvin temperatures are sensitive to the details of the interaction potentials between the colliding systems over an extended range of internuclear distances [1]. Here we explore the simple case of the elastic scattering at near-zero temperatures of a pair of sodium atoms for which apparently accurate interaction potentials can be constructed. We include the retardation effects (or Casimir corrections) and show that they change the scattering lengths and effective ranges by little, and move the shape resonances by small amounts. Finally, we compare our results to those obtained using a semiclassical derivation [2].

II. THEORY

A partial-wave expansion reduces the problem of elastic scattering by a potential $V(r)$ to the determination of the radial solutions $u_l(r)$ of the lth partial-wave equation

$$\left[\frac{d^2}{dr^2}+k^2-\frac{l(l+1)}{r^2}-U(r)\right]u_l(r)=0\ . \tag{1}$$

Here $k=\sqrt{2\mu E}/\hbar$ is the wave number, where E is the energy of the relative motion, μ is the reduced mass, and $U(r)=2\mu V(r)/\hbar^2$, where $V(r)$ is the (asymptotically vanishing) interatomic potential. The solutions must be regular and behave asymptotically as

$$u_l(r)\simeq A_l[s_l(kr)+c_l(kr)\tan\delta_l]\ ,\quad r\to\infty\ , \tag{2}$$

where A_l is a normalization constant, $s_l(x)=xj_l(x)$ and $c_l(x)=-xn_l(x)$ are the spherical Bessel and Neumann functions, and δ_l is the scattering phase shift. Alternatively, we can rewrite $u_l(r)$ as

$$u_l(r)\simeq A_l'\sin(kr-l\pi/2+\delta_l)\ ,\quad r\to\infty\ . \tag{3}$$

With A_l in Eq. (2) set equal to unity, a useful check is provided using the integral equation

$$\tan\delta_l=-\frac{1}{k}\int_0^\infty dr\, s_l(kr)U(r)u_l(r)\ . \tag{4}$$

The scattering by $V(r)$ is described by the phase shift δ_l, and a total elastic cross section may be defined by

$$\sigma_{\rm el}=\frac{4\pi}{k^2}\sum_{l=0}^{\infty}(2l+1)\sin^2\delta_l\ . \tag{5}$$

Sodium atoms in their ground states may approach along either of the potential-energy curves $V_g(r)$ and $V_u(r)$, corresponding, respectively, to the $X\,^1\Sigma_g^+$ and $a\,^3\Sigma_u^+$ states of Na_2. Elastic singlet and triplet cross sections may be defined by

$$\sigma_{\rm el}^{S,T}=\frac{4\pi}{k^2}\sum_{l=0}^{\infty}(2l+1)\sin^2\delta_l^{S,T}\ , \tag{6}$$

where S and T stand for singlet and triplet, respectively. The spin-change cross section is calculated from the singlet and triplet phase shifts by

$$\sigma_{\rm sc}=\frac{\pi}{k^2}\sum_{l=0}^{\infty}(2l+1)\sin^2(\delta_l^T-\delta_l^S)\ . \tag{7}$$

The low-energy scattering is dominated by the $l=0$ contribution. At values of k close to zero, the $l=0$ phase shift δ_0 can be represented by a power series expansion in k [3,4]:

$$k\cot\delta_0=-\frac{1}{a}+\tfrac{1}{2}r_e k^2+O(k^3)\ . \tag{8}$$

The parameters a and r_e, respectively, are the scattering length and the effective range. In the limit of low energies,

$$\sigma_{\rm el}^S=4\pi a_S^2\ ,\quad \sigma_{\rm el}^T=4\pi a_T^2\ ,\quad \sigma_{\rm sc}=\pi(a_T-a_S)^2\ , \tag{9}$$

where a_S and a_T, respectively, are the singlet and triplet scattering lengths. The scattering length corresponding to a potential $V(r)$ that decreases at large r as $-C_n/r^n$ has been obtained semiclassically by Gribakin and Flambaum [2] in the form

$$a=\bar{a}\left\{1-\tan\left[\frac{\pi}{n-2}\right]\tan\left[\Phi-\frac{\pi}{2(n-2)}\right]\right\}\ , \tag{10}$$

where

$$\bar{a}=\cos\left[\frac{\pi}{n-2}\right]\left\{\frac{\sqrt{2\mu C_n}}{\hbar(n-2)}\right\}^{2/(n-2)}\left[\frac{\Gamma\left[\frac{n-3}{n-2}\right]}{\Gamma\left[\frac{n-1}{n-2}\right]}\right] \tag{11}$$

and

$$\Phi=\frac{1}{\hbar}\int_{r_0}^{\infty}dr\sqrt{-2\mu V(r)}\ , \tag{12}$$

with $V(r_0)=0$. Gribakin and Flambaum have also shown that the number of bound states n_b is given by

$$n_b=\left[\frac{\Phi}{\pi}-\frac{n-1}{2(n-2)}\right]+1\ , \tag{13}$$

where [ ] indicates the largest integer. When [ ] in Eq. (13) is an integer, the scattering length is infinite, corresponding to the appearance of a new bound state.

The effective range r_e can be expressed in terms of the zero-energy solutions of the partial-wave equation (1). If $v_0(r)$ is the solution of Eq. (1) at $k=0$, with the potential taken to be zero everywhere, and normalized so that

$$v_0(r)=\frac{\sin(kr+\delta_0)}{\sin\delta_0}\quad\text{as } k\to 0\ , \tag{14}$$

and if $u_0(r)$ is normalized so that at large r

$$u_0(r)\sim v_0(r)\ , \tag{15}$$

then [4]

$$r_e=2\int_0^{\infty}dr[v_0^2-u_0^2]\ . \tag{16}$$

If a bound state with binding energy $|E_b|=\hbar^2\gamma^2/2\mu$ lies sufficiently near to the dissociation limit, a and r_e are related by [4]

$$-\frac{1}{a}=-\gamma+\tfrac{1}{2}r_e\gamma^2+\cdots\ . \tag{17}$$

III. POTENTIALS

The interaction potentials of two sodium atoms have been discussed by Zemke and Stwalley [5]. They have constructed an empirical Rydberg-Klein-Rees (RKR) potential curve for the $X\,^1\Sigma_g^+$ state using the spectroscopic constants of Babaky and Hussein [6] for vibrational levels between 0 and 44, and those of Barrow *et al.* [7] for $45\le v\le 62$. We extended the Zemke and Stwalley RKR curve with Babaky and Hussein data for $v=-0.5$ and -0.25 (see Table 3 in [6]). As noted by Zemke and Stwalley, we have to exclude the point at $r=12.429\,048$ Å (see Table III in [5]). We then have a RKR energy curve ranging from $4.1a_0$ to $30.0a_0$. Instead of using their exponential continuation for small distances, we completed the data by using a value from Konowalow, Rosenkrantz, and Olson [8] at $3.8a_0$, and then determined the short-range form at that first point ($r_{\min}=3.8a_0$)

$$V(r)=A\exp(-Br)\ ,\quad r\le r_{\min}\ , \tag{18}$$

with

$$A=V(r)\exp(Br)\big|_{r_{\min}}\quad\text{and}\quad B=-\left.\frac{\partial\ln V(r)}{\partial r}\right|_{r_{\min}}\ , \tag{19}$$

where $\partial V/\partial r|_{r_{\min}}$ is evaluated from a cubic spline fitting of the data points for $V(r)$.

The experimental data on the $a\,^3\Sigma_u^+$ state cover a less extensive range of r. We used the RKR values of Zemke and Stwalley [5] between $8.07a_0$ and $25a_0$, derived from the spectroscopic constants of Li, Rice, and Field [9]. Here again, we exclude a data point at $r=11.046\,804$ Å (see Table V in [5]). We extended this RKR curve in the short-range region with 11 points from Konowalow, Rosenkrantz, and Olson ranging from $3.8a_0$ to $7.5a_0$ (see Table III in [8]). The analytical form for the short-range region is the same as for the $X\,^1\Sigma_g^+$ state.

At large separations, $V_g(r)$ and $V_u(r)$ may be written as a sum of dispersion term r^{-n} and an exchange potential $V_{\rm exc}(r)$ which diminishes exponentially. Thus at large distances

$$V_{g,u}(r)=-\left[\frac{C_6}{r^6}+\frac{C_8}{r^8}+\frac{C_{10}}{r^{10}}\pm V_{\rm exc}(r)\right]\ . \tag{20}$$

For C_6, C_8, and C_{10} we used the values of Marinescu, Sadeghpour, and Dalgarno [10]. We give them in Table I and compare their values with other estimates. The value we adopted for C_6 is consistent with experimental measurements of the polarizability of sodium.

The exchange term $V_{\rm exc}(r)$ is very important to the determination of the spin-change cross section, and special care is needed if correct cross sections are to be obtained at low temperatures. Zemke and Stwalley [5] found the form $C\exp(-\beta r)$ to be a good approximation between $10a_0$ and $21a_0$, but it must become inadequate at larger r. Smirnov and Chibisov [11] have shown that if $\rho^2/2$ is the ionization potential of the atom in a.u., the exchange interaction has the asymptotic form

$$V_{\rm exc}(r)=\tfrac{1}{2}[V_u(r)-V_g(r)]=\tfrac{1}{2}Cr^{\alpha}\exp(-\beta r)\ , \tag{21}$$

where

$$\alpha=\frac{7}{2\rho}-1\ , \tag{22}$$

$$\beta=2\rho\ , \tag{23}$$

and $C(\rho)$ is given by

$$C(\rho)=\frac{A^4}{2^{1+1/\rho}}\frac{\Gamma(\frac{1}{2}\rho)}{\rho^{1+1/2\rho}}\times\int_0^1 dy(1-y)^{3/2\rho}(1+y)^{1/2\rho}\exp[(y-1)/\rho]\ , \tag{24}$$

where A is the amplitude of the valence electron wave function for large r,

$$\phi(r)=Ar^{1/\rho-1}e^{-\rho r}\ . \tag{25}$$

TABLE I. Dispersion coefficients in atomic units. We used the set of numbers from Ref. [10].

Source	C_6	C_8	C_{10}
Marinescu, Sadeghpour, and Dalgarno [10]	1472	111 877	11 065 000
Tang, Norbeck, and Certain [12]	1510±40	111 400±4,400	10 720 000±690 000
Maeder and Kutzelnigg [13]	1540	109 800	10 360 000
Konowalow and Rosenkrantz [14]	1680	164 000	
Li, Rice, and Field [9]	1637±33	157 000±4,700	

We determined A by using a model potential method [10] and obtained 0.751 16 in agreement with the value 0.751 recommended by Smirnov and Chibisov [11]. In Fig. 1 we compare the various values of $V_{\rm exc}(r)$ that have been suggested. There are significant differences. The *ab initio* calculations [8,14] and the empirical RKR curve [5] appear to be consistent neither with the fit recommended by Zemke and Stwalley [5] nor with the fit of Smirnov and Chibisov [11], from which we differ only slightly. However it is only the last *ab initio* point at $21a_0$ with which we disagree.

In Table II we list the parameters of the several recommended fits. Differences between the values derived from our fit and from those of Konowalow and Rosenkrantz [14], Li, Rice, and Field [9], and Zemke and Stwalley [5] become serious at separations beyond $20a_0$.

Retardation effects (or Casimir corrections) become important at very large distances. They affect the dynamical part of the potential, the dispersion terms. The exchange term, being an overlap of the atomic wave functions, is not modified by the time delay in the photon travel between the two atoms. The C_n/r^n terms take the form [15]

$$\frac{C_6}{r^6}+\frac{C_8}{r^8}+\frac{C_{10}}{r^{10}}\rightarrow f_6(r)\frac{C_6}{r^6}+f_8(r)\frac{C_8}{r^8}+f_{10}(r)\frac{C_{10}}{r^{10}}\ . \tag{26}$$

The functions $f_6(r)$, $f_8(r)$, and $f_{10}(r)$ have been calculated by Marinescu, Babb, and Dalgarno [15]. Asymptotically they decrease as r^{-1}.

The adopted hybrid potential curves of the singlet and triplet states are illustrated in Fig. 2. The differences between the curves with and without Casimir corrections are too small to be shown in Fig. 2.

Our adopted potentials yield a value of 6022.023 cm^{-1} for the dissociation energy of the $X\,^1\Sigma_g^+$ state, in close agreement with the value of 6022.03 cm^{-1} of Zemke and Stwalley [5] and of 6022.6±1.0 cm^{-1} of Barrow *et al.* [7]. For the $a\,^3\Sigma_u^+$ state, we obtained 174.083 cm^{-1} for the value of the dissociation energy, in close agreement with the value of 174.45±0.36 cm^{-1} of Li, Rice, and Field [9], and of 173.84 cm^{-1} using numbers from Zemke and Stwalley [5].

IV. ZERO ENERGY LIMIT

We solved Eq. (1) by the Numerov method, with automatic step size selection. We found that a more stable phase shift is obtained at low energies by substituting the solution into the integral Eq. (4) [16], rather than by fitting to the asymptotic form. We determined the scattering lengths and effective ranges by fitting the scattering phase shift δ_0 to the effective range expansion (8). We also calculated the scattering lengths using Eq.

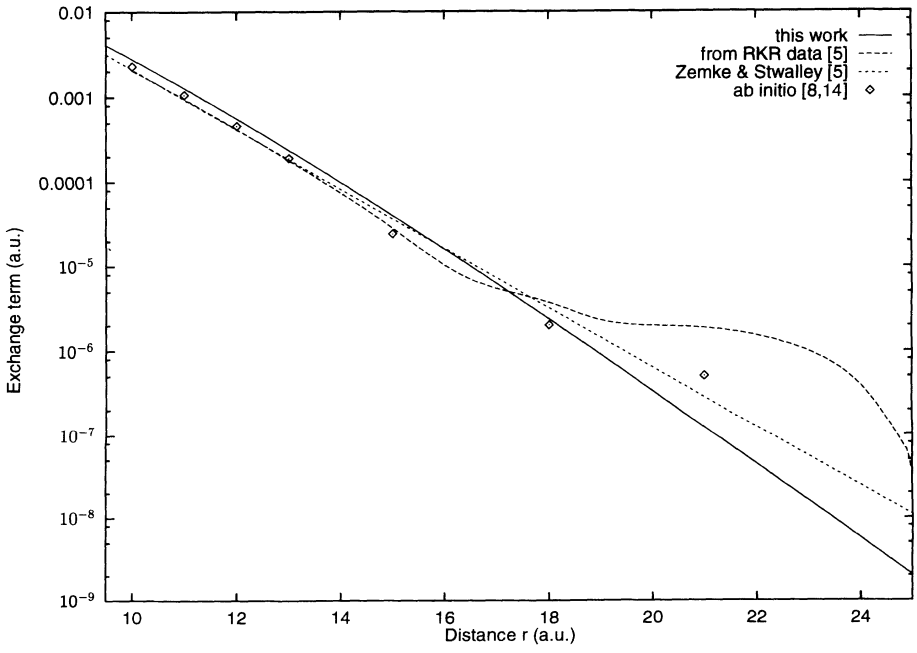

FIG. 1. Exchange term for Na_2: the RKR and Zemke and Stwalley fit are from [5].

TABLE II. Parameters for $V_{exc}(r)$, in a.u.

Source	$C/2$	α	β
This work	0.0123	4.693	1.229
Smirnov and Chibisov [11]	0.0125	4.59	1.252
Zemke and Stwalley [5]	7.0896	0.0	0.811 73
Li, Rice, and Field [9]	4.30	0.0	0.7662
Konowalow and Rosenkrantz [14]	0.345	0.0	0.649

TABLE III. Scattering lengths and effective ranges, in a.u.

State		a		r_e	
		Eq. (8)	Eq. (10)	Eq. (8)	Eq. (16)
$X\,^1\Sigma_g^+$	no retardation	34.936	35.615	184	187.5
	with Casimir	34.995		178	177.5
$a\,^3\Sigma_u^+$	no retardation	77.286	76.580	62	62.5
	with Casimir	77.352		61	60.7

(10), and effective ranges using Eq. (16). We adopted an atomic mass of 22.989 77 g/mole and a reduced mass of 20 953.879 58 electron masses, corresponding to the collision of two Na atoms.

The scattering lengths and effective ranges for the $X\,^1\Sigma_g^+$ and $a\,^3\Sigma_u^+$ states are presented in Table III. The close agreement between the calculations of a from Eqs. (8) and (10) and of r_e from Eqs. (8) and (16) confirms the accuracy of the numerical integrations of the partial-wave Eq. (1). The size of the scattering lengths and effective ranges is closely related to the position of the last vibrational bound states of the energy curves, as can be anticipated by inspection of Eqs. (10) and (13) or (17) which, consistent with Levinson's theorem, show that as the binding energy of the highest level tends to zero, the scattering length tends to $\pm$ infinity.

We have obtained the vibrational bound-state energies with zero angular momentum. They are listed in Table IV for the highest-lying levels, together with the experimental data [6,9]. We found 66 bound levels for the $X\,^1\Sigma_g^+$ state, and 16 bound levels for the $a\,^3\Sigma_u^+$ state. We confirmed that we had discovered all the bound levels by calculating their total number for each potential using formula (13) of Gribakin and Flambaum [2]. The table also includes the upward shifts in the energy levels that occur when the Casimir modification of the long-range interaction is taken into account. The shifts are everywhere less than 10^{-3} cm^{-1}.

The binding energies of the highest bound levels correspond to values of γ of 0.0824 and 0.0282 a.u., respectively, for the singlet and triplet states. The scattering lengths derived using Eq. (17) are not useful estimates because γr_e is large compared to unity, and neither value of γ is within the domain of convergence of Eq. (17).

The values obtained for the scattering lengths are determined by the quantity Φ. For the $X\,^1\Sigma_g^+$ state, $\Phi = 66\pi + 0.5506$, which implies that the potential well is just deep enough to acquire the last bound state and is far from acquiring another. Then $\tan(\Phi - \pi/8)$ from Eq. (10) with $n = 6$ lies on the positive branch and (10) gives a scattering length a smaller than the average value $\bar{a} = 42.3612 a_0$. For the $a\,^3\Sigma_u^+$ state, $\Phi = 15\pi + 2.8548$, which indicates that the potential well is close to accommodating an additional bound state. Then $\tan(\Phi - \pi/8)$ is on the negative branch, and (10) gives a larger value than $\bar{a}$.

The effective range depends on the overlap of the wave functions $v_0(r)$ and $u_0(r)$. Figure 3 shows the two wave functions for the singlet and triplet cases. The larger value of r_e for the $X\,^1\Sigma_g^+$ state comes from the larger lobe of $u_0(r)$ after $v_0(r)$ crosses the r axis, when compared to the $a\,^3\Sigma_u^+$ state.

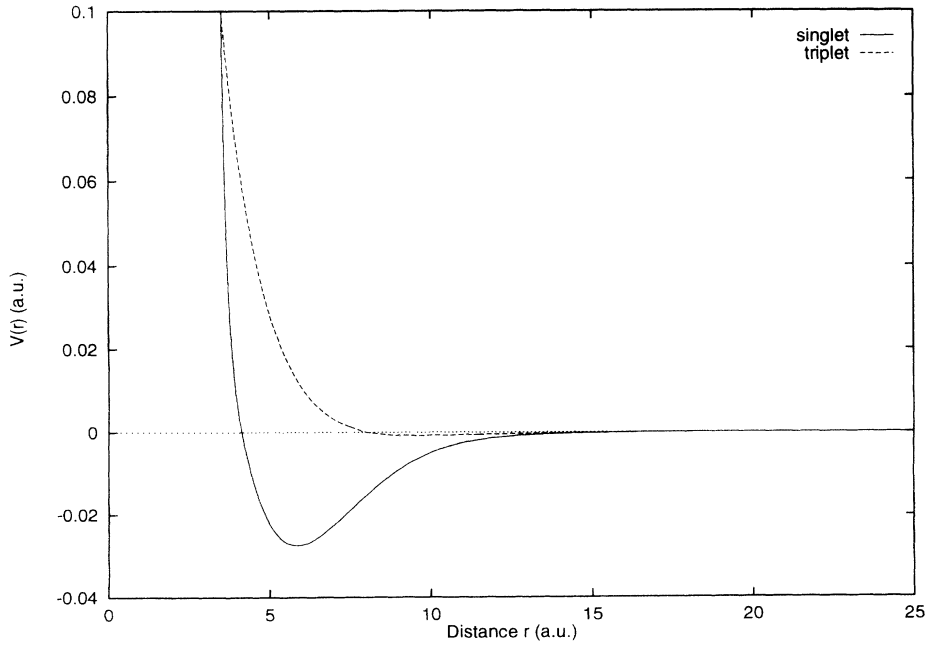

FIG. 2. The adopted potential energy curves of the $X\,^1\Sigma_g^+$ and $a\,^3\Sigma_u^+$ states of Na_2.

TABLE IV. Energies of $X\,^1\Sigma_g^+$ and $a\,^3\Sigma^+$ highest vibrational levels in cm^{-1}. Theory (a) is without retardation, and theory (b) is the retardation correction.

$X\,^1\Sigma_g^+$				$a\,^3\Sigma_u^+$			
		Theory				Theory	
v	Expt. [6]	(a)	(b)	v	Expt. [9]	(a)	(b)
⋮				⋮			
56	5940.2058	5940.1880	+1.229(−4)	6	5972.32	5972.1799	+3.247(−4)
57	5962.6055	5962.5881	+1.229(−4)	7	5984.68	5984.3137	+3.246(−4)
58	5980.8684	5980.8325	+1.229(−4)	8	5994.11	5994.5464	+3.239(−4)
59	5995.1549	5995.1109	+1.229(−4)	9	6003.57	6003.3288	+3.225(−4)
60	6005.7479	6005.7081	+1.229(−4)	10	6010.38	6010.5687	+3.251(−4)
61	6013.0942	6013.0439	+1.228(−4)	11	6016.01	6015.8063	+3.086(−4)
62	6017.8555	6017.8067	+1.254(−4)	12	6019.41	6019.2227	+2.363(−4)
63		6020.4606	+1.185(−4)	13		6021.1887	+1.516(−4)
64		6021.6504	+6.685(−5)	14		6022.0572	+6.779(−5)
65		6022.0011	+1.669(−5)	15		6022.2655	+7.902(−6)

The modification in the values of the scattering lengths and effective ranges due to the Casimir corrections are very small: 0.17% for a and 5.3% for r_e for the singlet, and 0.085% for a and 2.88% for r_e for the triplet. Equation (17) indicates qualitatively the effect of Casimir corrections. They lift the last bound-state levels and accordingly increase the scattering length, and by causing the potential to go to zero at a faster rate they produce smaller effective ranges.

Calculations of the triplet scattering length for Na atoms have been reported recently by Moerdijk and Verhaar [17]. Taking account of uncertainties in the $a\,^3\Sigma_u^+$ interaction potential, they concluded that $45a_0 < a_T < 185a_0$. Our value is $77.3a_0$.

V. HIGHER PARTIAL WAVES

With increasing energy, higher angular momentum waves contribute to the scattering. Figure 4 illustrates the variation with energy of the individual partial-wave cross sections for the $X\,^1\Sigma_g^+$ state. The total elastic cross section in units of a_0^2 is also presented in Fig. 4. The total cross section is constant at low velocities, where only s-wave scattering is significant. For very low energies, the s-wave cross section is constant and then increases slowly before decreasing at higher energies. This behavior can be explained by the values of a and r_e. For $l=0$, Eq. (6) becomes

$$\sigma_{\rm el}^S=\frac{4\pi}{k^2}\sin^2\delta_0=\frac{4\pi}{k^2+k^2\cot^2\delta_0}\ . \tag{27}$$

Using the effective range expansion and retaining terms up to the order of k^2, we find

$$\sigma_{\rm el}^S\simeq\frac{4\pi a^2}{(ka)^2+[1-\frac{1}{2}r_e ak^2]^2}$$

$$\simeq 4\pi a^2[1+ak^2(r_e-a)]\ . \tag{28}$$

Since (r_e-a) and a are positive, Eq. (28) is consistent with the calculated behavior. The s-wave cross section tends to decrease with increasing energy, but the decrease is overcome by higher partial-wave contributions which initially increase with energy from zero before passing through maxima and decreasing. Oscillations occur through the addition of a small number of partial waves. The $l=1$ partial wave starts to contribute at $\log_{10}E\simeq -8.5$, corresponding to a temperature of 1 mK, and higher l becomes important at larger energies. Sharper structures are due to shape resonances. The most prominent is the f-wave resonance corresponding to a quasibound state trapped by the $l=3$ centrifugal barrier. A second resonance is found for $l=7$. The positions in the energy spectrum and widths of these resonances are given in Table V. However, the large contribution of the partial wave $l=4$ is due to a near approach of the phase shift to a multiple of $\pi/2$ at $\log_{10}E=-6.7$, as shown in Fig. 5.

We illustrate in Fig. 6 the similar calculations for the $a\,^3\Sigma_u^+$ state. The same general features are found. The s-wave cross section tends to decrease with increasing energy, but the decrease is overcome by higher partial-wave contributions. We do not observe the small increase in the s-wave cross section before the decrease because (r_e-a) is negative while a is positive. Here the $l=1$ partial wave begins to contribute at a very low energy ($\log_{10}E\simeq -10.5$) corresponding to a temperature of 10 μK. The higher partial waves become more important around $\log_{10}E\simeq -8.5$ or 1 mK. A small resonance appears in the $l=6$ partial wave. Its position and width are given in Table V. Here also, the important contribution

TABLE V. Resonance energies and widths.

State	l	$V_{exc}(r)$	$\log_{10}E_\Gamma$	E_Γ (10^{-9} a.u.)	Γ (10^{-10} .u.)
$X\,^1\Sigma_g^+$	3	no retardation	−7.303	49.77	161.5
		with Casimir	−7.302	49.89	164.4
	7	no retardation	−6.6454	226.26	3.402
		with Casimir	−6.6450	226.46	3.416
$a\,^3\Sigma_u^+$	6	no retardation	−6.6571	220.24	54.90
		with Casimir	−6.6568	220.39	55.10

TABLE VI. Spin-charge rate coefficients. The numbers in brackets denote multiplicative powers.

$\log_{10}[T$ (K)]	$\mathcal{R}$ ($cm^3 s^{-1}$)
−6	6.7[−13]
−5	2.1[−12]
−4	8.2[−12]
−3	4.4[−11]
−2	1.7[−10]
−1	2.1[−10]
0	3.5[−10]
1	4.6[−10]

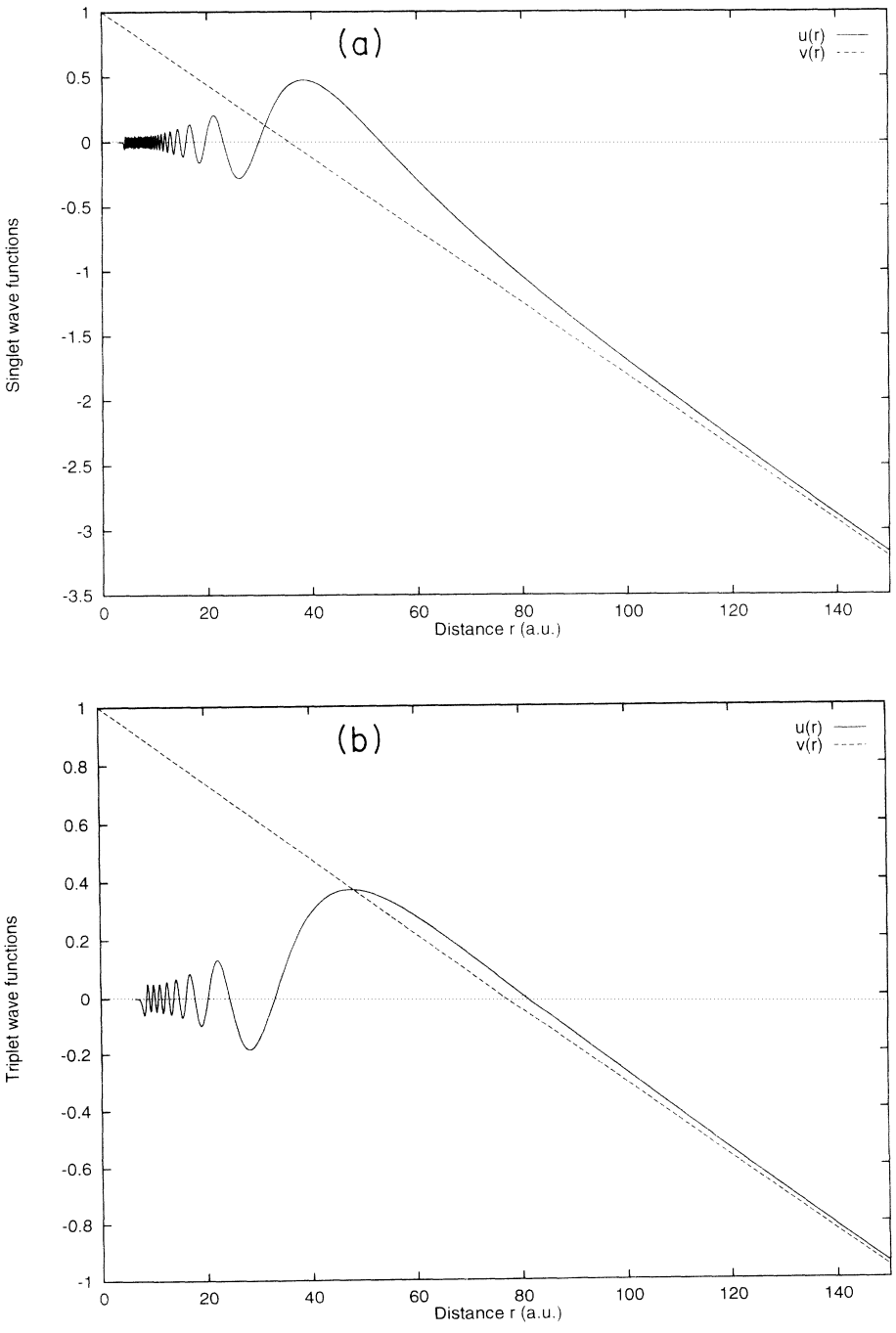

FIG. 3. The wave functions $u_0(r)$ of the $X\,^1\Sigma_g^+$ (a) and $a\,^3\Sigma_u^+$ (b) states of Na_2 for $k \to 0$, together with the zero-potential solutions $v_0(r)$. The scattering length is the intersection of $v_0(r)$ with the r axis.

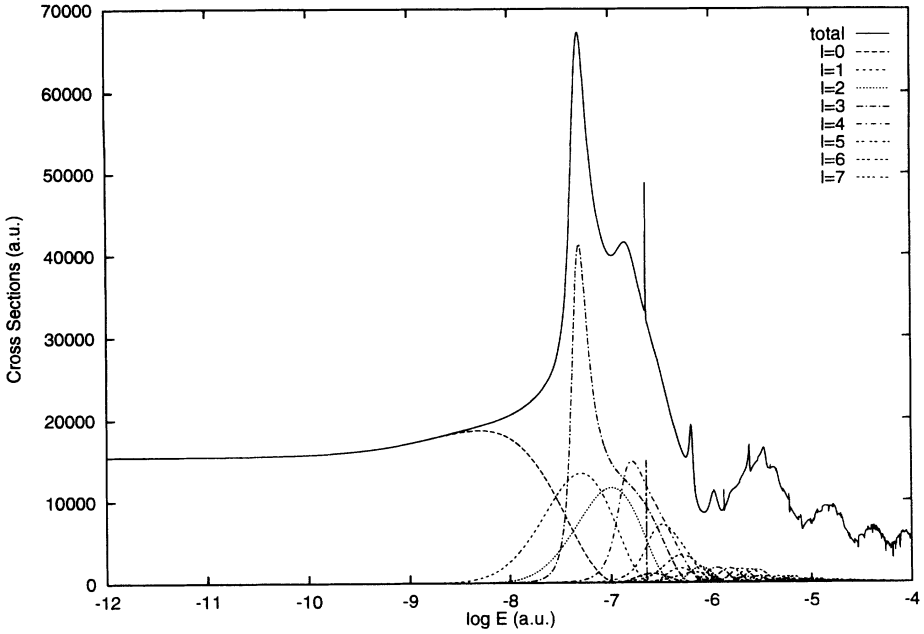

FIG. 4. The individual partial-wave cross sections and the total cross section for the scattering in the $X\,^1\Sigma_g^+$ state as functions of collision energy. The logarithmic scales in Figs. 4–8 are to base 10.

from the $l=2$ partial wave is due to the phase shift approaching a multiple of $\pi/2$ at $\log_{10}E=-7.5$.

The spin-change cross section is shown in Fig. 7. The contributions of both the singlet and triplet resonances are visible, and the same general description is valid.

The effect of the Casimir corrections on the shape resonances is shown in Table V. They move the resonances by very small amounts, and cause little change in the width Γ.

VI. TEMPERATURE DEPENDENCE

We assume the velocity distribution is Maxwellian characterized by a kinetic temperature T, and we define mean elastic and spin-change cross sections by

$$\bar{\sigma}(T)=(k_BT)^2\int_0^\infty dE\,E\sigma(E)\exp(-E/k_BT)\ . \quad (29)$$

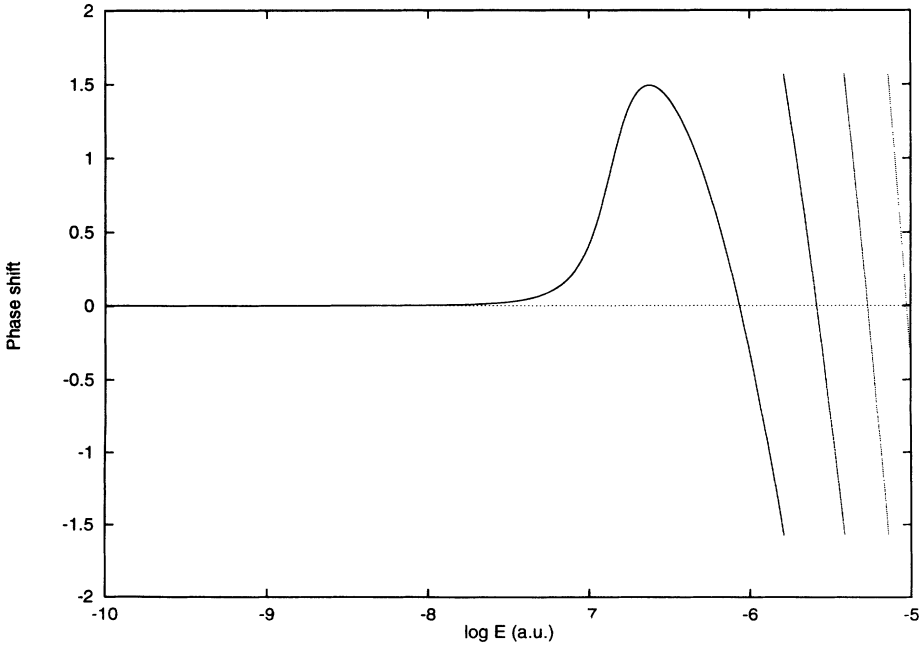

FIG. 5. Elastic scattering phase shift as a function of energy for the partial wave $l=4$ of the $X\,^1\Sigma_g^+$ state.

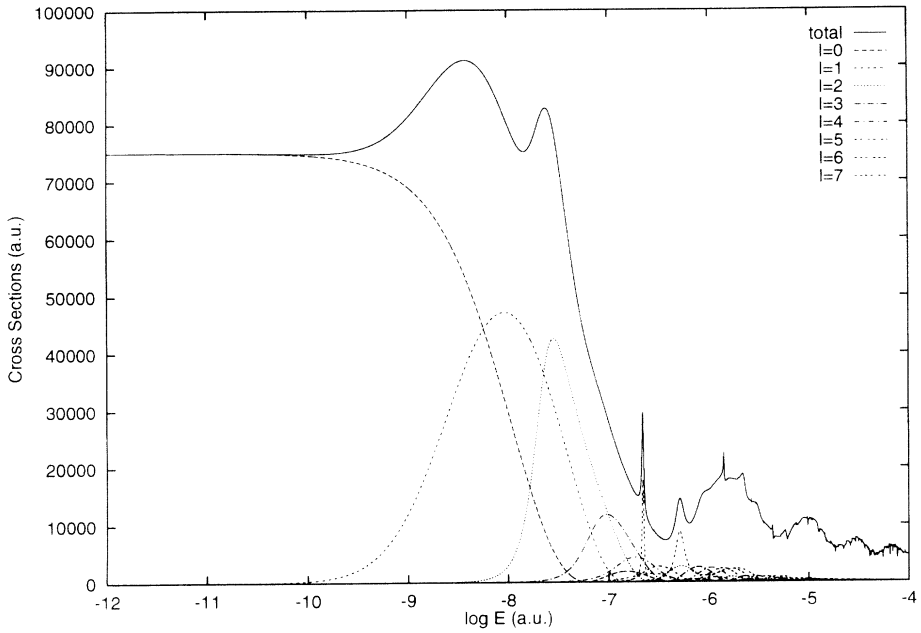

FIG. 6. The individual partial-wave cross sections and the total cross section for the scattering in the $a\,^3\Sigma_u^+$ state as functions of collision energy.

The corresponding rate coefficients are given by

$$\mathcal{R} = \left[\frac{8k_B T}{\pi\mu}\right]^{1/2} \bar{\sigma}_{sc}(T) \,. \tag{30}$$

Values of the mean cross sections in units of a_0^2 are shown in Fig. 8 for T up to 10 K, and values of the corresponding spin-change rate coefficient in $cm^3\,s^{-1}$ are listed in Table VI. The cross sections are large and, because of the sensitivity to the details of the interaction potentials [1], they are very uncertain at low temperatures. At higher temperatures, where many partial waves contribute, the predictions are more reliable. The influence of higher partial waves begins to become evident at temperatures as low as 1 mK for the triplet case and 10 mK for the singlet and spin-change cases, as shown in Fig. 8.

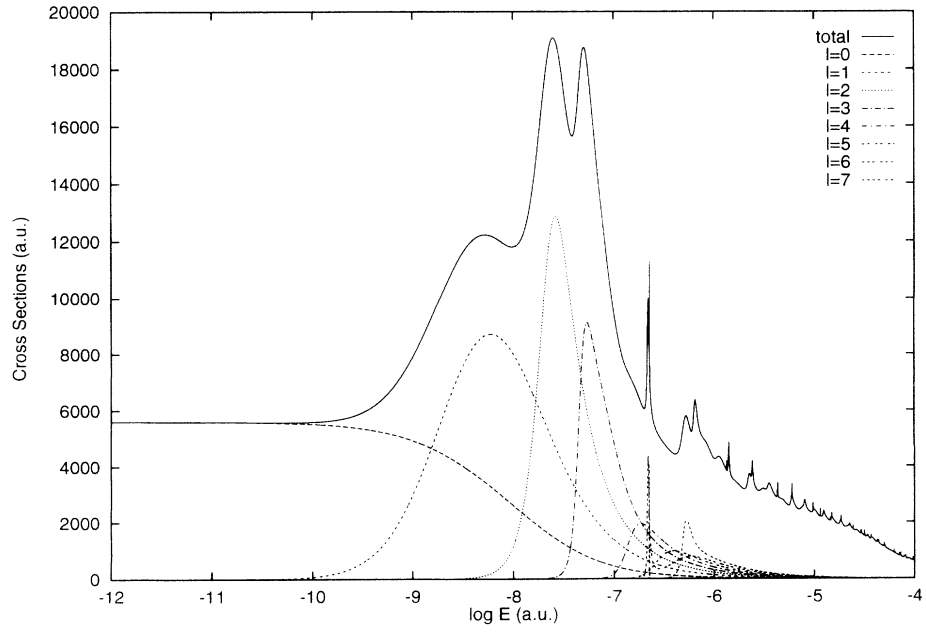

FIG. 7. The individual partial-wave cross sections and the total cross section for the spin-change process as functions of collision energy.

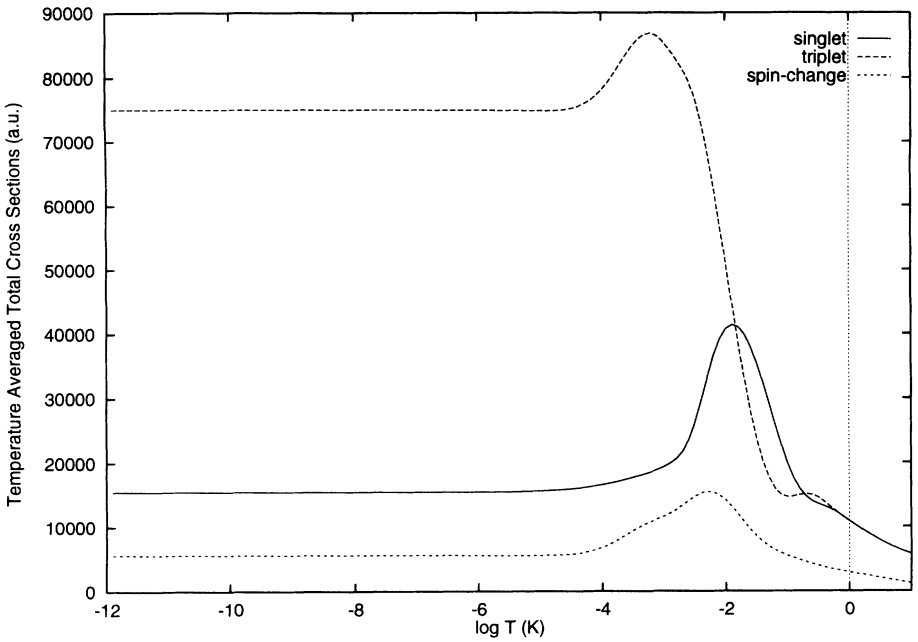

FIG. 8. The thermally averaged elastic and spin-change cross sections as functions of temperature.

VII. CONCLUSIONS

The elastic cross sections for the collision of two Na atoms at ultralow temperatures are sensitive to the details of the interaction potentials [1] but are probably very large, of the order of 10^{-13} cm^2. Below 1 mK, the collisions are dominated by s-wave scattering, but higher partial waves contribute at higher temperatures. Shape resonances, trapped within the centrifugal barrier, impose structure on the cross sections. The scattering lengths are predicted to be positive for both singlet and triplet scattering. The effects of the Casimir corrections are very small: the scattering lengths increase by 0.1%, the effective ranges decrease by 3.0%, and the shape resonances are moved slightly in energy.

ACKNOWLEDGMENTS

Dr. M. Marinescu provided valuable advice and remarks regarding the Casimir corrections. This work was supported by the Division of Chemical Sciences, Office of Basic Energy Sciences, Office of Energy Research, U.S. Department of Energy.

[1] R. Côté. A Dalgarno, and M. J. Jamieson, Phys. Rev. A **50**, 399 (1994).
[2] G. F. Gribakin and V. V. Flambaum, Phys. Rev. A **48**, 546 (1993).
[3] O. Hinckelmann and L. Spruch, Phys. Rev. A **3**, 642 (1971).
[4] C. J. Joachain, *Quantum Collision Theory* (North-Holland, Amsterdam, 1975).
[5] W. T. Zemke and W. C. Stwalley, J. Chem. Phys. **100**, 2661 (1994).
[6] O. Bababy and K. Hussein, Can. J. Phys. **67**, 912 (1989).
[7] R. F. Barrow J. Verges, C. Effantin, K. Hussein, and J. D'Incan, Chem. Phys. Lett. **104**, 179 (1984).
[8] D. D. Konowalow, M. E. Rosenkrantz, and M. L. Olson, J. Chem. Phys. **72**, 2612 (1980).
[9] L. Li, S. F. Rice, and R. W. Field, J. Chem. Phys. **82**, 1178 (1985).
[10] M. Marinescu, H. R. Sadeghpour, and A. Dalgarno, Phys. Rev. A **49**, 982 (1994).
[11] B. M. Smirnov and M. I. Chibisov, Zh. Eksp. Teor. Fiz. **48**, 939 (1965) [Sov. Phys. JETP **21**, 624 (1965)].
[12] K. T. Tang, J. M. Norbeck, and P. R. Certain, J. Chem. Phys. **64**, 3063 (1976).
[13] F. Maeder and W. Kutzelnigg, Chem. Phys. **42**, 95 (1979).
[14] D. D. Konowalow and M. E. Rosenkrantz, J. Phys. Chem. **86**, 1099 (1982).
[15] M. Marinescu, J. F. Babb, and A. Dalgarno, Phys. Rev. A (to be published).
[16] R. Côté and M. J. Jamieson (unpublished).
[17] A. J. Moerdijk and B. J. Verhaar, Phys. Rev. Lett. **93**, 518 (1994).